Water Quality Monitoring and Mapping using Rapidly Deployable Sensor Nodes

by

Mohamed Abdelwahab

Bachelor of Science
Arab Academy for Science, Technology and Maritime Transport, 2019

Submitted in Partial Fulfillment of the Requirements

for the Degree of Master of Science in

Mechanical Engineering

College of Engineering and Computing

University of South Carolina

2023

Accepted by:

Austin R.J. Downey, Director of Thesis

Sourav Banerjee, Reader

Ann Vail, Dean of the Graduate School

Abstract

Efficient and continuous monitoring of water quality parameters plays a pivotal role in responding to pollution incidents and ensuring the safety of both human consumption and ecological resources. This research introduces an affordable and dependable in-situ water quality sensor package designed for seamless continuous monitoring, providing essential data to facilitate informed decision-making in water resource management. The sensor package enables comprehensive on-site assessment of key water characteristics, including pH, temperature, turbidity (measured in NTU), and total dissolved solids (TDS, measured in ppm). Spatial interpolation techniques, specifically Kriging, are employed to extrapolate variable values at unobserved locations based on nearby measurements.

To guarantee the system's durability and reliability, the microcontroller, electronic components, and battery are encased within a sealed transparent PVC tube to safeguard against water exposure. An outer water-resistant cap securely seals the non-submerged portion of the probes, augmented by an additional layer of resilient resin to provide enhanced protection against water ingress during operation. Furthermore, the integration of Unmanned Aerial Vehicles (UAVs) equipped with electromagnetic deployment mechanisms represents a significant advancement in data collection. Embedded within UAV systems, this technology streamlines the deployment of sensor packages in previously inaccessible or challenging terrains. The electromagnetic deployment mechanism ensures precise and focused sensor placement, a crucial factor in Kriging, which relies heavily on accurate data points for spatial interpolation. This innovation accelerates data collection and enhances data reliability, fundamentally

reshaping our capacity for informed decision-making in safeguarding the environment and effectively managing resources.

To mitigate sinking and simplify retrieval, flotation equipment is incorporated into the package design. Rigorous benchtop testing confirms the precision of the pH, TDS, and temperature sensors. A comparative analysis with industrial sensors, notably those from VIVOSUN renowned for their accuracy, reveals minimal error percentages between our sensor package and these industry-standard counterparts. Specifically, the error percentages for pH, TDS, and temperature sensors are recorded at 1.34%, 5.23%, and 0.81%, respectively, underscoring the reliability and accuracy of the sensor package in field-based water parameter monitoring. Additionally, a comprehensive power management assessment demonstrates that the in-situ water quality sensor package is capable of continuous operation for an impressive duration of 32 hours and 48 minutes.

Field testing of the in-situ water quality sensor package involved collecting data from six strategically positioned sampling points within a stationary pond. We employed Kriging for spatial interpolation to generate water quality maps, which illustrated a uniform distribution of measured parameters across the sampled area. Notably, pH values ranged from 6 to 6.7, turbidity varied between 11 and 18 NTU, TDS values spanned from 44 to 51 ppm, and the temperature fluctuated between 22.8 and 24.6 degrees Celsius. These findings highlight the sensor package's potential for monitoring water quality in larger surface water bodies, providing an invaluable tool for environmental stewardship and resource management.

Table of Contents

List of Tables

List of Figures

Chapter 1

Introduction

As a vital and irreplaceable natural resource, water is the foundation of various ecosystems and is fundamentally essential for sustaining life on Earth. However, the increasing impact of industrial and technological developments has resulted in significant water quality degradation, posing a severe threat to human health and the environment. While effective, traditional water quality monitoring methods are often time-consuming, costly, and require significant effort. In response, researchers have been exploring using automated systems to provide continuous, real-time monitoring of various water quality parameters and enable early warning of environmental threats.

The in-situ water quality sensor package is an automated system that continuously monitors several water quality parameters, including pH, total dissolved solids (TDS), turbidity, and temperature [2] [11]. These parameters are crucial in determining the suitability of water for human consumption, the survival of aquatic organisms, and the presence of pollutants [14]. For example, pH levels can indicate the presence of contaminants; turbidity can affect the taste and harbor harmful microorganisms. For instance, high TDS can indicate harmful pollutants, and temperature can affect aquatic organisms and indicate certain pollutants. Monitoring these parameters in real-time allows for quick detection of potential threats to water quality[15]. By providing real-time water quality monitoring, the in-situ sensor package enables water resource managers to make informed decisions quickly and accurately [13] [30] [4].

This research presents a low-cost, high-quality in-situ water quality sensor package that monitors various parameters such as pH, TDS, turbidity, and temperature in a stationary pond [2] [11]. The study utilizes the Kriging method to predict the values of unsampled areas within the pond, thereby providing a comprehensive understanding of water quality distribution [31] [22]. To enhance the efficiency of data collection, the study employs a hexacopter drone equipped with an electromagnetic deploying mechanism to deploy the sensor package. This innovative approach not only ensures the precise placement of sensors but also minimizes human intervention in the data collection process [10], as well as enabling access to inaccessible and remote locations [9][24] [32]. In addition to the continuous monitoring provided by the in-situ sensor package, the study employed a data logger to systematically collect and record the results of the testing, ensuring comprehensive data capture for further analysis[21]. Figure 1.1 illustrates the methodology employed in this study, which aims to address the challenges associated with traditional water quality monitoring methods, known for their high costs, labor-intensive procedures, incomplete monitoring, and data reporting delays.

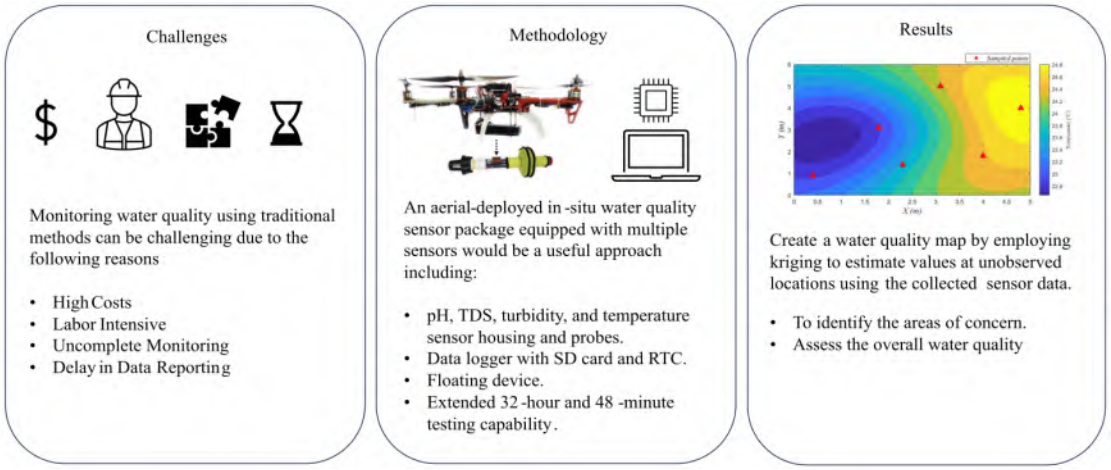

Figure 1.1: Visual summary of key findings and methodology.

The research findings presented in this study underscore the remarkable capabilities of employing an in-situ sensor package in tandem with the kriging method[7]. This combined approach offers a level of accuracy and reliability that is crucial for achieving real-time monitoring[33] of diverse water quality parameters [15]. Among the parameters assessed, this comprehensive system effectively tracked pH levels, Total Dissolved Solids (TDS), turbidity, and temperature[2] across six distinct sampling points situated within a stationary pond. This not only provides valuable insights into the water's condition but also sheds light on the transformative potential that automated sensing systems have in the field of water quality monitoring and management [3] [1].

One of the key innovations of this study lies in the visualization of its findings, as the data has been skillfully translated into informative maps[3]. These maps serve as powerful tools for enhancing comprehension, allowing viewers to easily grasp the intricate patterns of water quality variations across the monitored area[33]. By graphically representing the data researchers can readily identify regions that may require particular attention or intervention.

Chapter 2

Methodology

In-situ water quality sensor packages are advanced embedded systems that fundamentally change water quality monitoring by providing real-time measurement capabilities[33]. These packages can be directly deployed in water bodies or attached to floating surfaces, enabling continuous monitoring and recording of water quality parameters without labor-intensive manual sampling and laboratory analysis [13]. The in-situ water quality sensor package as shown in Figure 2.1 offers several notable advantages for water quality monitoring. Firstly, it enables real-time monitoring, allowing immediate access to crucial data[27]. The sensors incorporated in the package are highly accurate and can measure various parameters, including pH, TDS (Total Dissolved Solids), temperature, and turbidity [2] [11]. This accuracy ensures reliable data for detailed analysis and assessment. Another advantage is the cost-effectiveness of the package compared to traditional monitoring methods[25] [12]. It eliminates the need for frequent manual sampling and laboratory analysis, reducing associated costs and time-consuming processes[24]. Additionally, the package allows for remote access to the data, enabling convenient monitoring and management[21].

The design process of the in-situ water quality sensor package, including the selection of waterproof housing[26], integration of essential components like sensors, data logger, microcontroller, and PCB, and careful consideration of environmental conditions, is essential to ensure reliable and efficient water quality monitoring. The utilization of a UAV (Unmanned Aerial Vehicle)[12], a hexacopter drone equipped with an electromagnetic deploying mechanism to deploy the sensor package[8], enhances

the overall efficiency of data collection and enables access to inaccessible locations[32]. This meticulous design process guarantees a highly functional and dependable sensor package capable of withstanding harsh aquatic environments and facilitating continuous real-time monitoring of water quality parameters [4][30][5].

Overall, the in-situ water quality sensor package is valuable for convenient and effective water quality monitoring. It provides access to accurate data, is cost-effective, and is easy to install and maintain.

The design process is critical in ensuring reliable performance and robust functionality, making it an indispensable asset in water quality management.

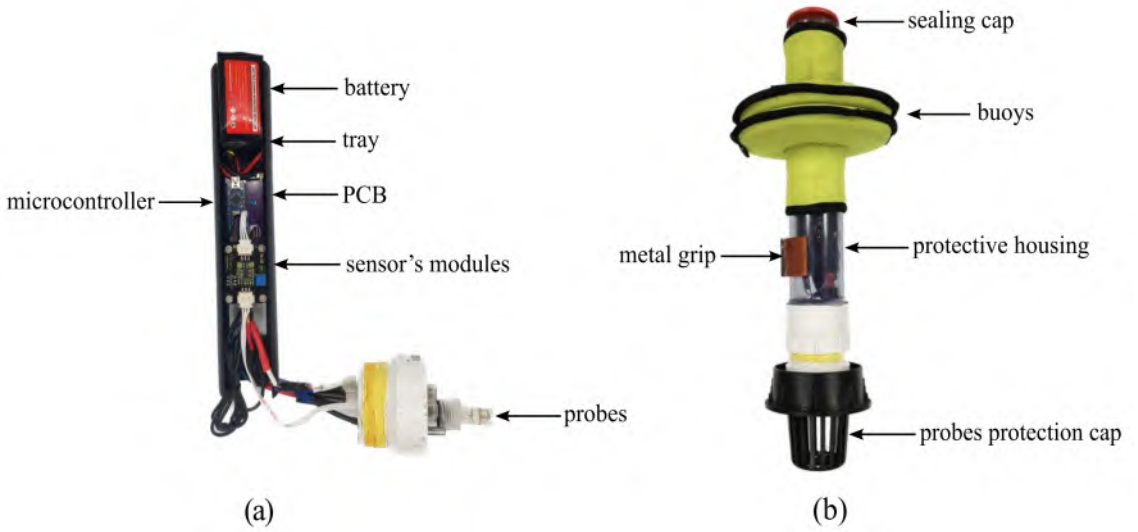

Figure 2.1: (a) Revealing the internal components of the sensor package, (b) View of the fully assembled in-situ water quality sensor package.

2.1 UAV-deployable sensor

The utilization of Unmanned Aerial Vehicles (UAVs) has emerged as a crucial component in the field of water quality monitoring. UAVs provide a unique and efficient approach to deploying in-situ water quality Sensor packages in diverse aquatic environments. These remotely piloted aircraft offer the flexibility and accessibility required to reach challenging areas[32]. Integrating the in-situ water quality sensor package with the UAV platform enables the collection of adequate real-time data with rapid response timesa[27]. Moreover, UAVs play a crucial role in ensuring precise sensor package placement, which is essential for the accuracy of the kriging process. By utilizing the exceptional navigational abilities of UAVs, we achieve remarkable precision in deploying these sensors, resulting in reliable data points that significantly enhance the accuracy and reliability of kriging estimates[7].

A multi-propeller hexacopter drone [13] with a built-in electromagnetic deploying system enables the In-Situ Water Quality Sensor Package deployment as shown in Figure 2.3. This system plays a crucial role in lifting and releasing the sensor package. A vital component of this mechanism is a strategically positioned metal grip on the side of the sensor package. Following the magnetic attraction principle, this grip interacts with the ferromagnetic component within the UAV's electromagnetic system. The magnetic field causes the metal grip on the sensor package to respond, resulting in an attractive force. The electromagnetic system controls this action by adjusting the polarity of the metal grip. Once the UAV reaches the desired location, the actuator generates the appropriate action, causing the metal grip on the sensor package to either attach or detach from it, thereby initiating a controlled deployment into the water body as displayed in Figure 2.2.

The deployment, guided by the actuator's precision, ensures that the sensor package enters the water smoothly and efficiently, with the anchor mechanism playing a

crucial role in maintaining its stability and alignment once it is submerged. Additionally, strategically placed buoys provide additional stability and buoyancy to the system, further enhancing its performance in aquatic environments[34].

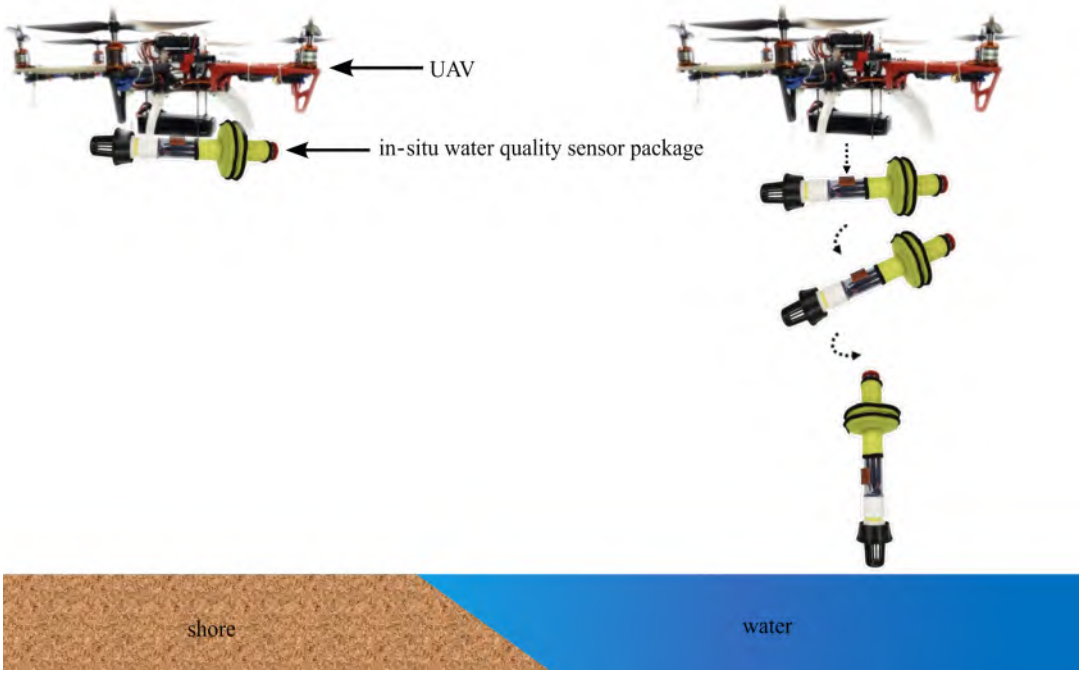

Figure 2.2: Applied method of deploying the sensor package using the UAV.

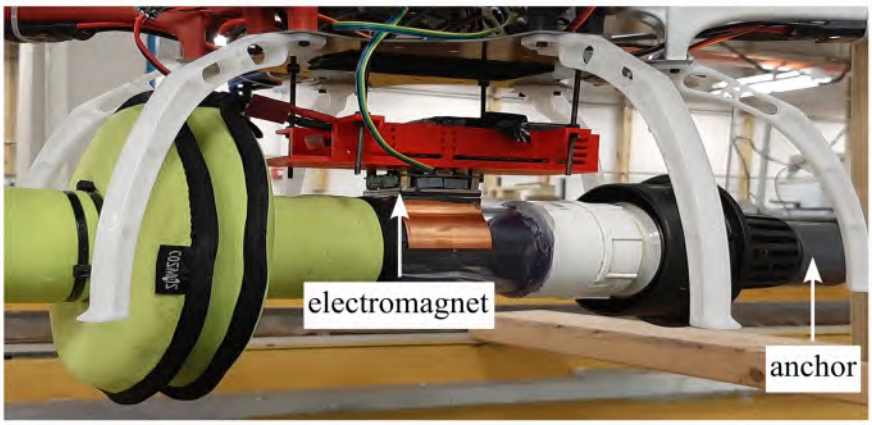

Figure 2.3: Robust sensor deployment mechanism with a stable anchor.

Integrating the GPS (Global Positioning System) with the UAV is instrumental in achieving precise placement of the sensor package, particularly within the framework of kriging analysis. By leveraging the advanced capabilities of GPS technology, the UAV accurately determines its position, enabling the sensor package to be deployed with exceptional spatial precision at the desired coordinates.

The GPS is a reliable guide for the UAV's navigation and waypoint guidance, ensuring adherence to predefined flight paths at designated deployment areas[17][19]. This seamless integration of GPS technology significantly enhances the reliability and precision of the sensor package deployment process, thus making a valuable contribution to the acquisition of high-quality data vital for water quality monitoring and analysis, especially in optimizing the accuracy of kriging models[20].

There are several essential characteristics in the chosen UAV. First, it is a multi-propeller hexacopter, which provides stability and maneuverability, allowing for precise control during the flight process. Additionally, the drone provides a significant payload capacity, enabling the integration of the In-Situ Water Quality Sensor Package without affecting the drone's flight performance.

Furthermore, the drone offers an efficient flight system, allowing for extended operational periods and the ability to cover large areas. This efficiency enables effective water quality monitoring. Moreover, the UAV uses a sophisticated remote controller with a joystick and control buttons, allowing the operator to navigate the drone precisely and easily during flight operations[28].

2.2 Sealed and Protective Frame

The sensor package has been meticulously engineered to excel in demanding and waterlogged environments, as exemplified in Figure 2.4. This design prioritizes both waterproof integrity and operational efficiency.

To begin with, a transparent PVC tube boasting a 2.5-inch outer diameter and a 2-inch inner diameter was carefully chosen as the primary housing component. This material not only provides exceptional waterproofing but also transparency, allowing for visual inspection of the internal components.

The protective housing plays host to a multitude of critical components, including the various sensors, electronic devices, and the battery. To ensure a watertight assembly, a PVC coupling, equipped with external threads, was securely affixed to one end of the PVC tube using PVC cement. This coupling serves as the connecting link to the sensor package cap, which securely holds the sensor probes, as indicated in Figure 2.4 (a).

To further enhance its resistance to water ingress, a layer of water-resistant resin was expertly applied to the surface of the cap. This additional layer acts as a formidable barrier against moisture, reinforcing the overall water resistance of the sensor package.

Simultaneously, the opposing end of the PVC tube was sealed with a meticulously crafted tube closure. This closure is not just an afterthought but an essential component, guaranteeing complete waterproofing and ensuring the utmost security of the package's internal electronics.

The outer frame of the sensor package was deliberately designed with versatility in mind, facilitating its attachment to floating surfaces or buoys. This feature permits the sensor package to remain buoyant and afloat on the water's surface, thereby expanding its potential applications.

Moreover, recognizing the vulnerability of the sensor probes, a probe protection cap was thoughtfully integrated into the design. This cap serves as a guardian, shielding the probes from potential damage and prolonging their operational lifespan.

In conclusion, the sensor package's design and choice of materials ensure it works reliably even in harsh water conditions. This has been proven in real-world applications as mentioned in [34].

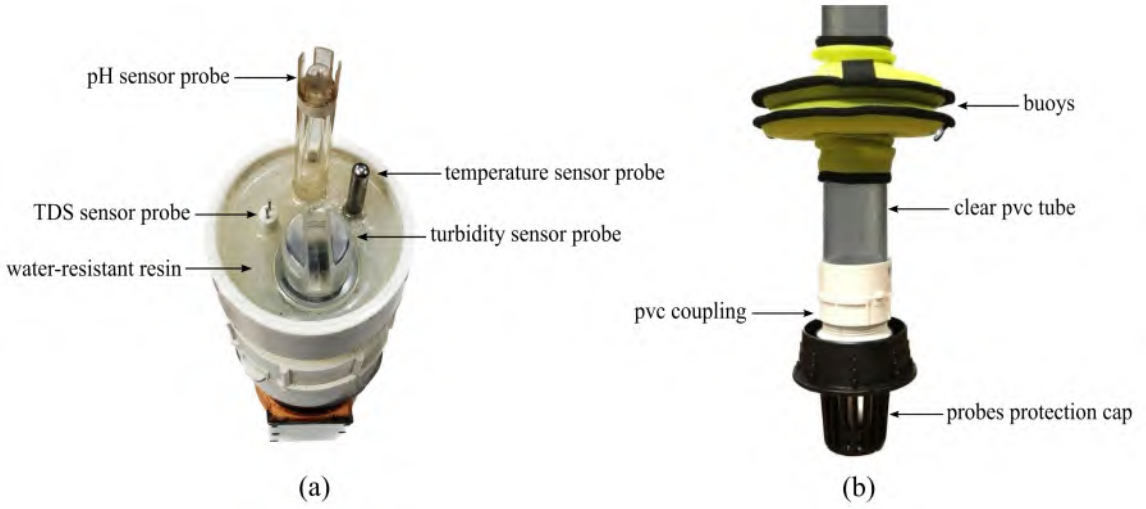

Figure 2.4: (a) Unveiling the sensor package probes, (b) Protective outer frame to ensure sealing of the sensor package.

2.3 Electronic Components

Electronic components serve as the brain of in-situ water quality sensor packages, responsible for collecting, processing, and transmitting data to the end user. Real-time monitoring and analyzing water quality parameters would be impossible without these components. Therefore, careful selection and integration of electronic components were crucial during the design process to ensure the sensor package's accuracy, reliability, and durability.

To provide a visual representation of the intricate electronic components involved, A comprehensive block diagram has been displayed in Figure 2.5, offering an insightful glimpse into the interconnected nature of these critical elements:

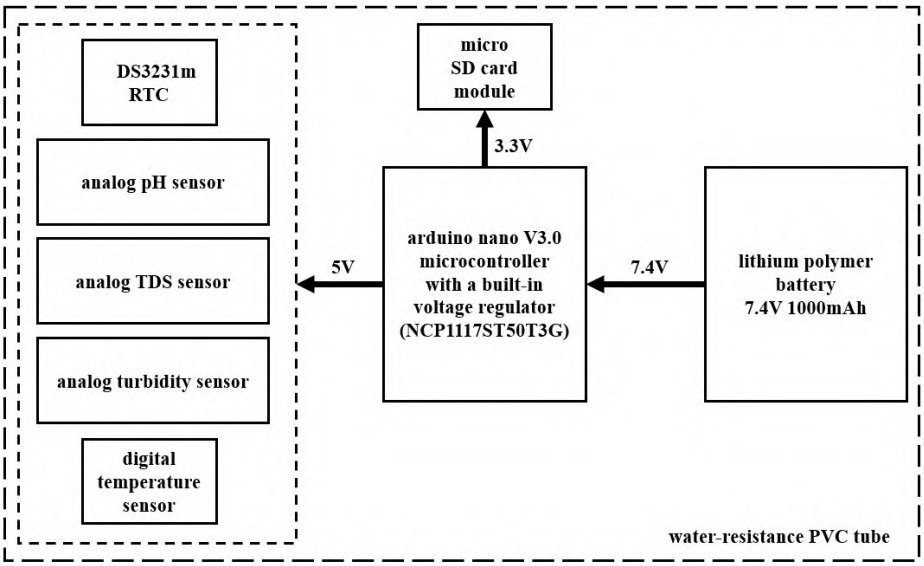

Figure 2.5: Block diagram displaying the internal components of the sensor package.

The diagram visually reveals the complex interplay of electronic components within the sensor package, emphasizing its reliable performance. For a more in-depth exploration of these components, each element has been examined in dedicated subsections, providing comprehensive insights into their functions and interactions.

Sensors

Among the sensors selected, the Atlas Scientific pH meter as shown in Figure 2.6 was crucial in the water quality sensor package[13] [25] [12]. This high-accuracy analog pH sensor is designed to measure the pH of liquids, making it an essential tool for monitoring water quality parameters. In addition, the Atlas Scientific pH sensor is exceedingly power-efficient, consuming less than one milliampere (mA) of current during regular operation, and can operate within a voltage range of 3.3 V to 5 V.

Figure 2.6: Atlas scientific pH sensor module.

The pH value, which falls from 0 to 14, is determined by first converting the received analog signal into a digital signal using an advanced analog-to-digital converter (ADC). This digitized signal is then processed by the onboard microcontroller employing equation 2.1 to deliver accurate results.

$$pH = (-5.6548 \times V) + 15.509 \tag{2.1}$$

The turbidity sensor is a crucial component of the sensor package, playing a pivotal role in assessing water quality [25] [12] [2]. The selected turbidity sensor model was V1.0, manufactured by Keystudio as displayed in Figure 2.7 [11]. Its crucial function quantifies the amount of scattered light resulting from suspended particles in the water, including silt, sediment, algae, and other organic and inorganic particles, indicating the water quality. The turbidity sensor consists of an infrared-emitting diode (IRED) that serves as an emitter and a phototransistor that functions as a receiver, converting detected photons into electrical signals. The resulting electrical signals are typically displayed as voltage readings, converted into standardized turbidity units such as NTU (Nephelometric Turbidity Units).

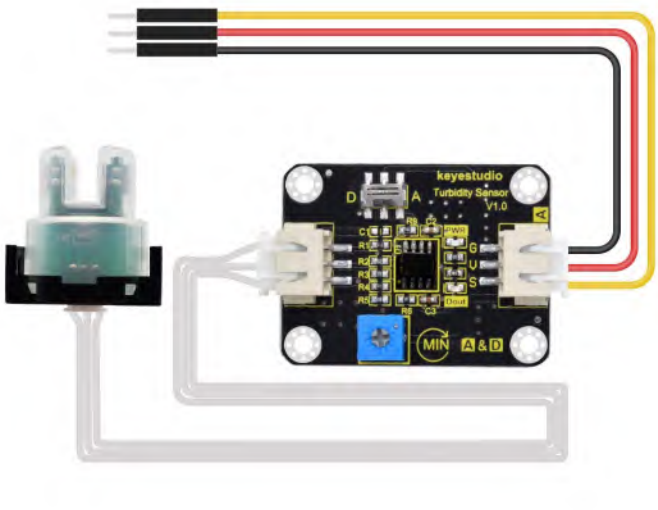

Figure 2.7: Unveiling Keystudio turbidity sensor module.

To achieve this conversion, we performed a calibration process using the map function in the sensor package algorithm. The map function was implemented by comparing the output voltage of the turbidity sensor to known NTU values ranging from 0 to 100 in a linear relationship, allowing for precise and accurate turbidity measure-

ments. The map function was implemented by comparing the output voltage of the turbidity sensor to known NTU values ranging from 0 to 100 in a linear relationship, allowing for precise and accurate turbidity measurements. This function converts the raw electrical signals the turbidity sensor produces into standardized turbidity units. This calibration process using the map function in the sensor package algorithm made it a valuable tool for water quality assessment.

In addition, the sensor package for this study included the TDS (Total Dissolved Solids) sensor, explicitly utilizing the V1.0 model developed by Keystudio as shown in Figure 2.8 [2] [11]. The TDS sensor operates within an operating voltage range of 3.3V to 5V and offers a measuring range of 0 to 1000 ppm (Parts Per Million). This sensor employs the principle of electrical conductivity to measure the concentration of dissolved solids in water. The TDS sensor includes a probe featuring two electrodes immersed in the water sample. By applying a voltage across these electrodes, the dissolved ions within the water facilitate the flow of electrical current between them.

Figure 2.8: Displaying Keystudio TDS sensor module.

Consequently, the measured conductivity of the water is directly proportional to the concentration of dissolved solids present in the sample, enabling a comprehensive assessment of dissolved solids concentration in a water sample. The TDS value was determined using Equation 2. The equation was formulated to convert the measured voltage from the TDS sensor into corresponding TDS values.

$$TDS = (133.42 \times (V)^3 - 255.86 \times (V)^2 + 857.39 \times V) \times 0.5 \tag{2.2}$$

The DS18B20 temperature sensor was the final sensor included in the package [11]. It is a digital sensor known for its broad temperature measurement range of -55 °C to 125 °C, providing an accuracy of ±0.5°C within the range of -10°C to +85°C. Among its advantages are low power consumption and a compact design. The sensor as shown in Figure 2.9 is utilized in various fields, including industrial automation, environmental monitoring, and scientific research, where precise and reliable temperature measurements are essential. To guarantee seamless communication with the sensor, it was connected to the system using the 1-Wire protocol, which required the incorporation of a pull-up resistor.

Figure 2.9: Presenting DS18B20 temperature sensor.

Data Logger

The data logger, equipped with an SD card module and RTC (Real-Time Clock)[6], plays a crucial role in our in-situ water quality sensor for this study. It efficiently records and stores data from various sensors within the package, including pH, TDS, turbidity, and temperature as illustrated in Figure2.10. In this research, the micro SD card module was a crucial component of the data logger in the sensor package. Its compact size as shown in Figure 2.11 (b) and low power consumption at 3.3V facilitated seamless communication between the microcontroller and the SD card, enabling efficient data storage and retrieval within the data logger system.

The In-Situ sensor package utilizes the DS3231M IC as the Real-Time Clock as displayed in Figure 2.11 (a), ensuring accurate timekeeping for precise data logging. This IC boasts several advantageous features, including low power consumption for efficient operation, extended battery life, and optimized overall performance of our water quality monitoring system. It also offers battery backup support, guaranteeing continuous timekeeping even during power failures or interruptions, preventing data loss, and ensuring uninterrupted monitoring of water quality parameters.

Moreover, the DS3231M IC incorporates a built-in temperature sensor, enabling it to compensate for oscillator frequency variations caused by temperature changes within a wide range of -40 Celsius to +85 Celsius. This temperature compensation feature ensures reliable and accurate timekeeping, even in environments with varying temperature conditions. Furthermore, the DS3231M IC offers flexibility in time representation, functioning in 24-hour and 12-hour formats with an AM/PM indicator.

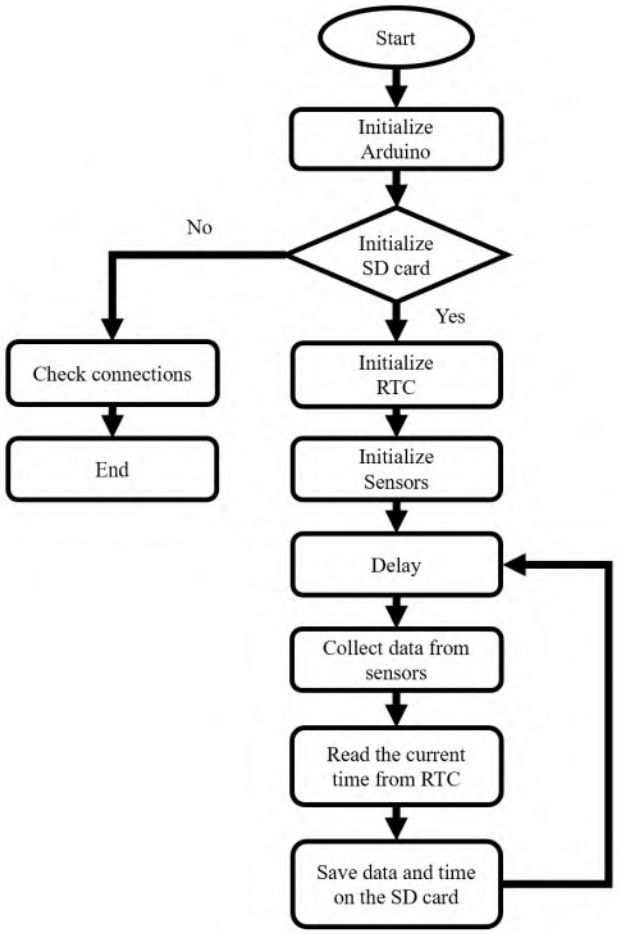

Figure 2.10: Sensor package deployment mission algorithm breakdown.

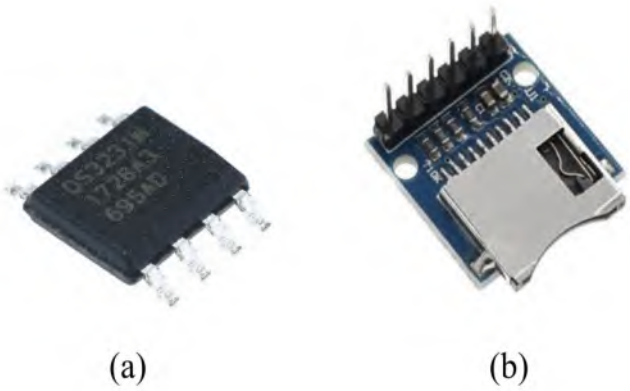

Figure 2.11: Displaying the data logger components (a) DS3231M, (b) micro SD card.

Microcontroller

The Arduino Nano, featured in Figure2.12, serves as the cornerstone of our sensor package's operations, overseeing control functions and complex computations. Its compact design, based on the ATmega328P microcontroller, is a perfect fit for our space-constrained project, offering versatility and efficiency. Operating at a standard 5 volts with a recommended range of 7 to 12 volts, it strikes the right balance between power requirements and performance. Its remarkable energy-saving capabilities make it ideal for power-conscious applications, Furthermore, its affordability makes it a prime choice for projects aiming to achieve exceptional performance without exceeding budget constraints.

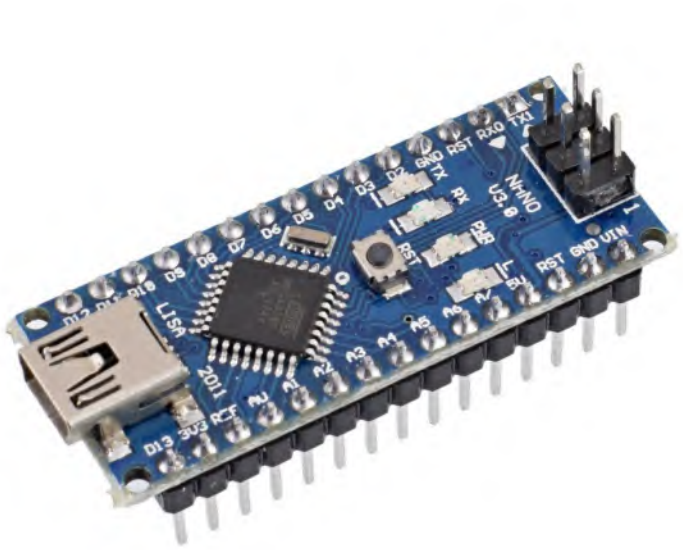

Figure 2.12: Arduino nano the microcontroller used in the sensor package.

2.4 PCB Design

Designing the PCB for the in-situ water quality sensor package posed challenges, mainly due to size constraints. The team created a compact PCB to fit all components within the limited space as displayed in Figure 2.13. Starting with a schematic diagram as shown in Figure 2.14, they established electrical connections and ensured functionality while considering size and compatibility during component selection. The team employed manual routing techniques to precisely control traces and component placement to address the constraints, achieving an optimized layout. Figure 2.15 illustrates the designed PCB.

In addition to these technical considerations, the team conducted thorough research to source the most suitable electronic components, taking into account their size, power consumption, and compatibility. This meticulous component selection process was critical to ensuring the sensor package's performance met the project's requirements without compromising on the compact design.

Figure 2.13: Compact PCB integrating the electronic components for the in-situ water quality sensor package.

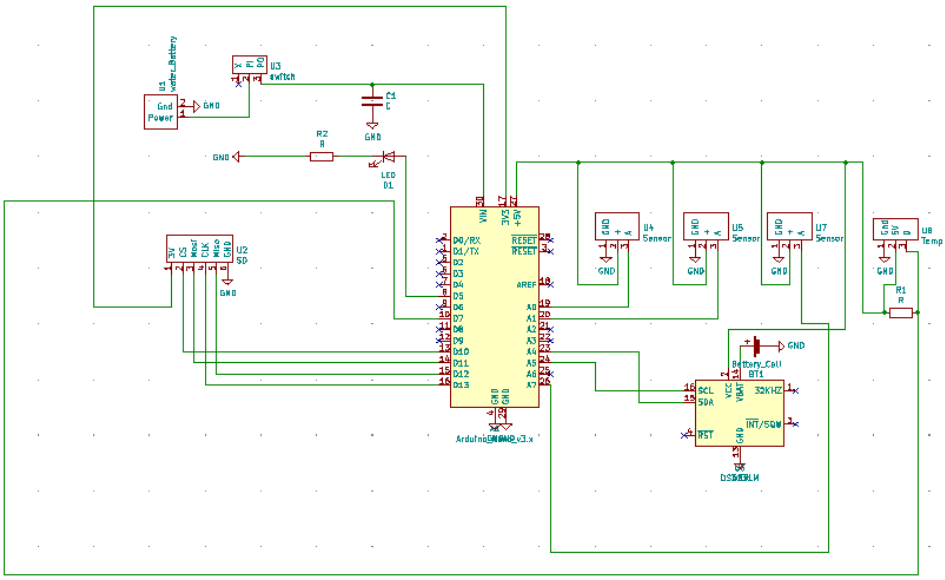

Figure 2.14: Schematic diagram of the in-situ water quality sensor circuit.

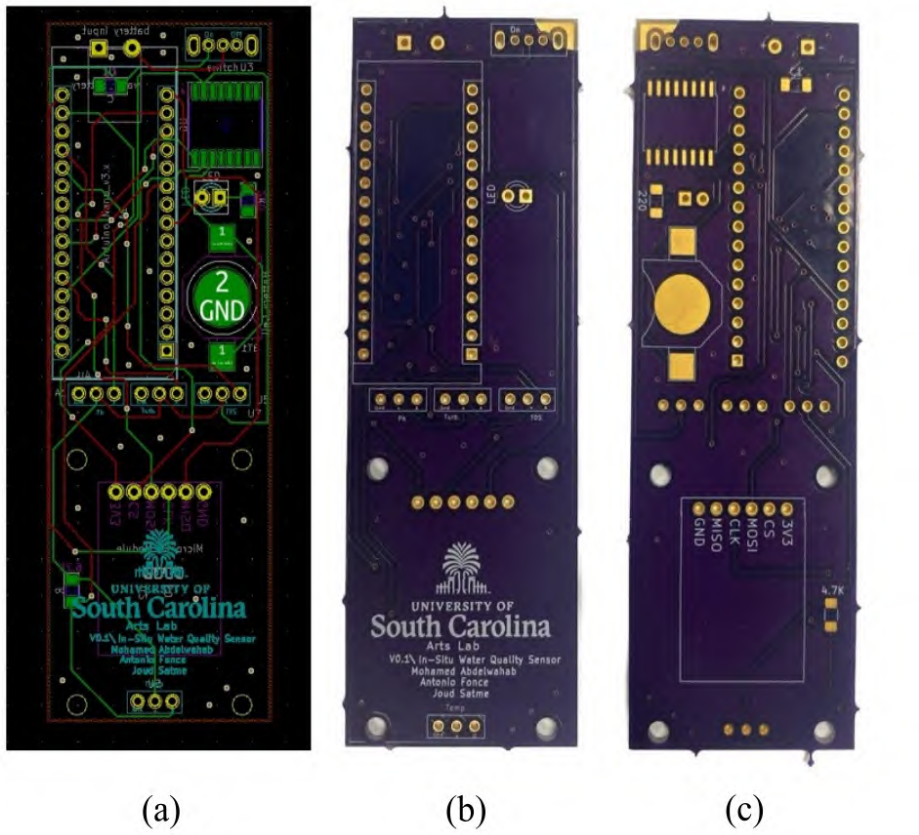

Figure 2.15: (a) Designed Footprints of the PCB, (b) Front Side of the PCB, and (c) Back Side of the PCB for the In-Situ Water Quality Sensor Package.

2.5 Kriging

For the semi-variogram model associated with the ordinary kriging algorithm, we selected a Spherical semi-variogram as illustrated in Figure 2.16. Literature suggests that it is the optimal choice for describing the distribution of a solvent in a fluid body [18].

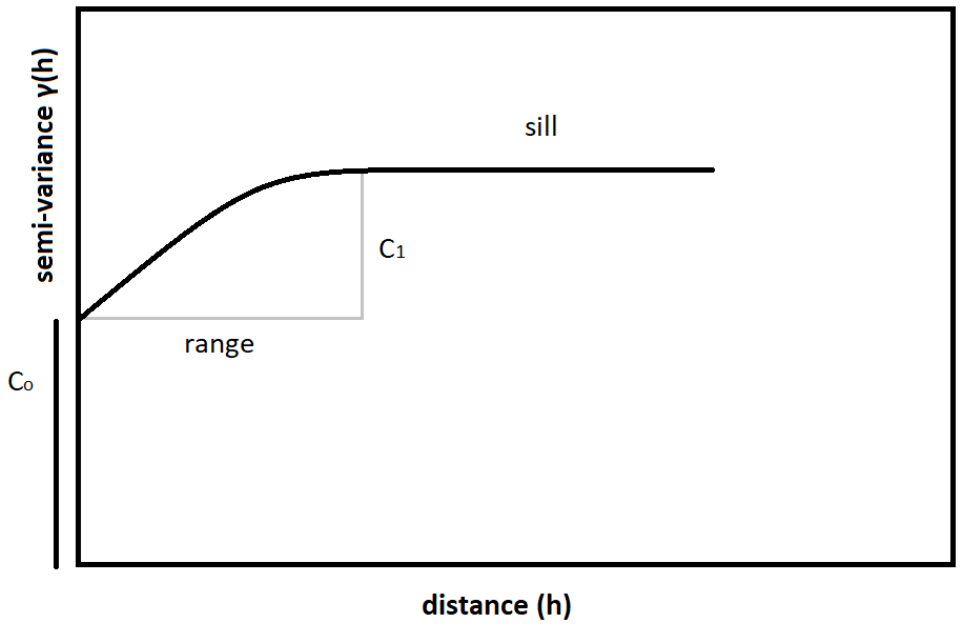

Figure 2.16: Kriging variogram model.

The use of kriging equips us with several built-in methods to minimize the inherent variance of measurements, thereby enhancing the accuracy of the data field. Kriging procedures take advantage of the 'nugget' of the variogram, which effectively functions as a noise filter and a range parameter that limits the influence of outliers to specific regions, preserving the accuracy of the entire model.

Kriging proves to be a valuable method for comprehending the distribution of physical properties in bodies of water, surpassing traditional approaches [23]. When combined with high sample rates from deployable sensor packages, Kriging offers significant insights into spatial correlations among data sets.

Continuous data collection using Kriging leverages in-situ water quality sensor packages to enhance water quality monitoring. These sensors gather data on pH, TDS (Total Dissolved Solids), turbidity, and temperature, generating a dynamic dataset that captures variations in water quality.

Spatial interpolation, a crucial aspect of Kriging, estimates water quality parameters at unmeasured locations using geostatistical techniques [16]. By considering the spatial correlation between nearby observations, this method incorporates the underlying spatial structure of the data. Strategic deployment of in-situ water quality sensors across the study area captures a representative sample of the water body. Combined with Kriging, continuous measurements from these sensors create high-resolution maps that illustrate the spatial distribution of water quality parameters, aiding in identifying hotspots, areas of concern, and spatial trends for targeted monitoring and management strategies.

The semi-variogram is a fundamental component used in conjunction with the ordinary kriging procedure, as described by equations 2.3, 2.4 and 2.5.

$$\gamma = C_0 + C\left(1.5\left(\frac{h}{a}\right) - 0.5\left(\frac{h}{a}\right)^3\right) \tag{2.3}$$

$$Z(s_i) = m(s_i) + e(s_i) \tag{2.4}$$

$$Z(\mathbf{x}) = \sum_{k=0}^{K} \beta_k f_k(\mathbf{x}) + \epsilon(\mathbf{x}) \tag{2.5}$$

This approach offers cost-effectiveness by deploying in-situ water quality sensors for ongoing data collection across locations, reducing the need for costly, manual sampling. Integrated with Kriging, it enables real-time monitoring, generating water quality maps for identifying the areas of concern and assessing the overall water quality for decision-making.

2.6 Optimal Sensor Placement Methods

Optimal sensor placement methods aim to determine the locations where sensors should be deployed to achieve efficient data collection with the fewest sensors. The goal is to strategically position sensors in a way that maximizes the quality and coverage of data while minimizing the number of sensors deployed.

In the context of water quality monitoring, optimal sensor placement offers a range of advantages, including improved data quality, cost efficiency, early contaminant detection, and environmental conservation, thereby enabling more effective and sustainable water quality monitoring programs crucial for safeguarding water resources and public health. Several methods and strategies, such as random placement, grid-based placement, and cross-validation, are employed to achieve effective data collection.

Random Sensor placement

Random sensor placement is a practical method for monitoring stationary bodies of water in uniform environments. It involves deploying sensors arbitrarily, without a structured grid or optimization.

This approach is valued for its simplicity and operational efficiency, making it suitable when water quality is expected to be relatively uniform across the entire area of interest and no specific spatial variations are critical. While simple, it can still provide valuable data for monitoring, particularly in cost-effective scenarios that don't require comprehensive coverage or meticulous planning.

In our study, we employ random sensor placement for its simplicity and suitability for testing a stationary water body with uniform conditions.

Grid-based placement

Grid-based placement is one method that can be effective for monitoring stationary water bodies. This approach involves deploying sensors across a structured grid pattern, ensuring a systematic and uniform distribution of monitoring points. Grid-based placement is particularly suitable when the goal is to achieve consistent and evenly distributed data across the entire water body. It is often used for long-term monitoring and when there is a good understanding of the water body's characteristics.

Cross-validation

Cross-validation optimizes sensor placement by dividing available data into training and testing sets. It objectively measures the effectiveness of sensor configurations by systematically excluding portions of data in each iteration, including the valuable "leave-one-out" approach. This iterative process refines sensor locations, enhancing strategy precision by identifying areas contributing the most valuable data. This critical process ensures efficient, accurate data collection, vital for understanding and safeguarding water resources and public health.

Chapter 3

Validation

3.1 Numerical Validation

The research team conducted a comprehensive numerical validation to assess the precision of kriging as an interpolation method for estimating pH values in a simulated lake. They generated a synthetic lake to mimic the distribution of pH values across its surface, as depicted in Figure 3.1. By selecting specific observation points from the synthetic lake, they ensured the representation of diverse areas and pH variations.

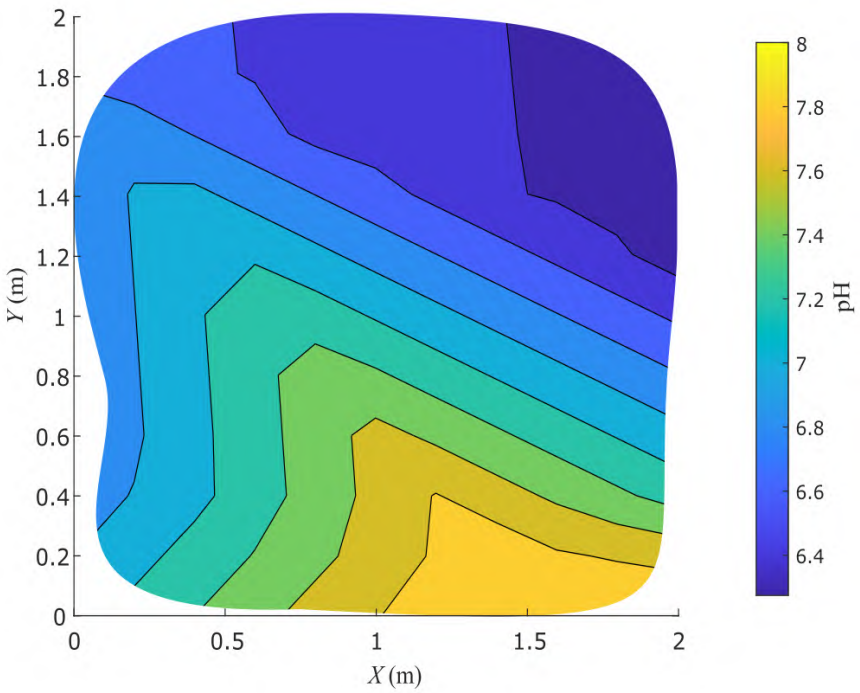

Figure 3.1: pH variance throughout the fabricated lake.

The research team employed kriging interpolation in eight iterations, each with varying numbers of sampled data points ranging from 4 to 30.

This approach allowed for the accurate estimation of pH values at locations that were not directly sampled. The resulting findings are beautifully visualized in Figures 3.2 and 3.3, offering a clear representation of the interpolated pH values across the study area.

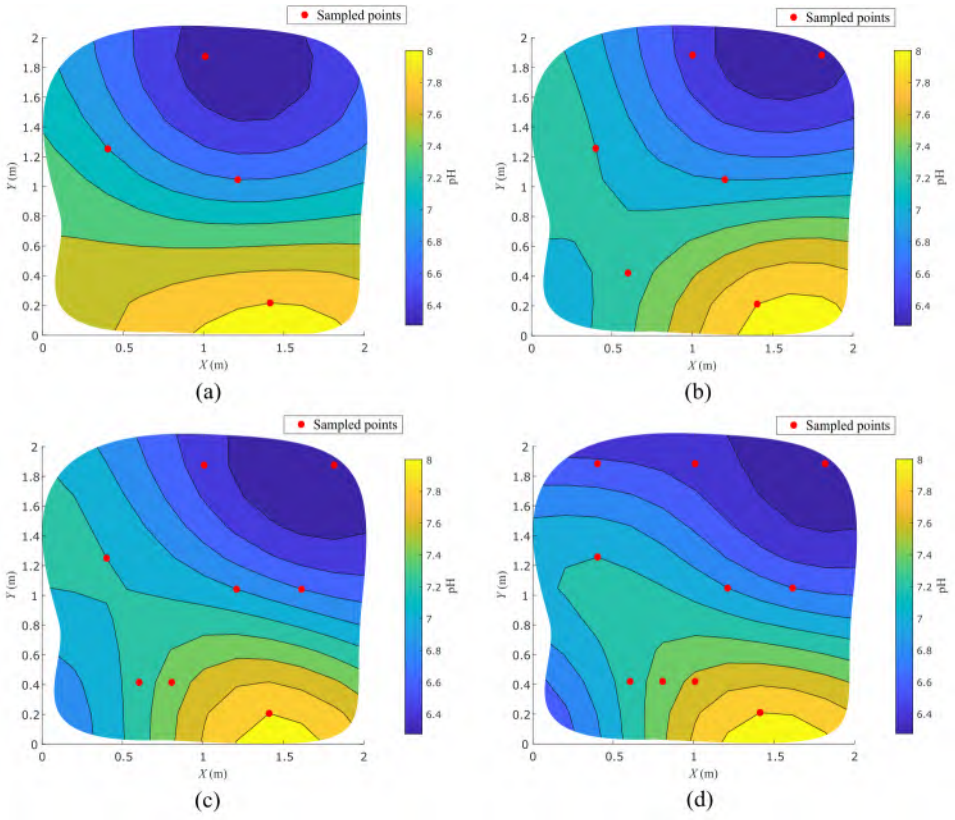

Figure 3.2: Assessing the kriging method accuracy to the fabricated lake by increasing the sampled points showing (a) 4 points, (b) 6 points, (c) 8 points, (d) 10 points.

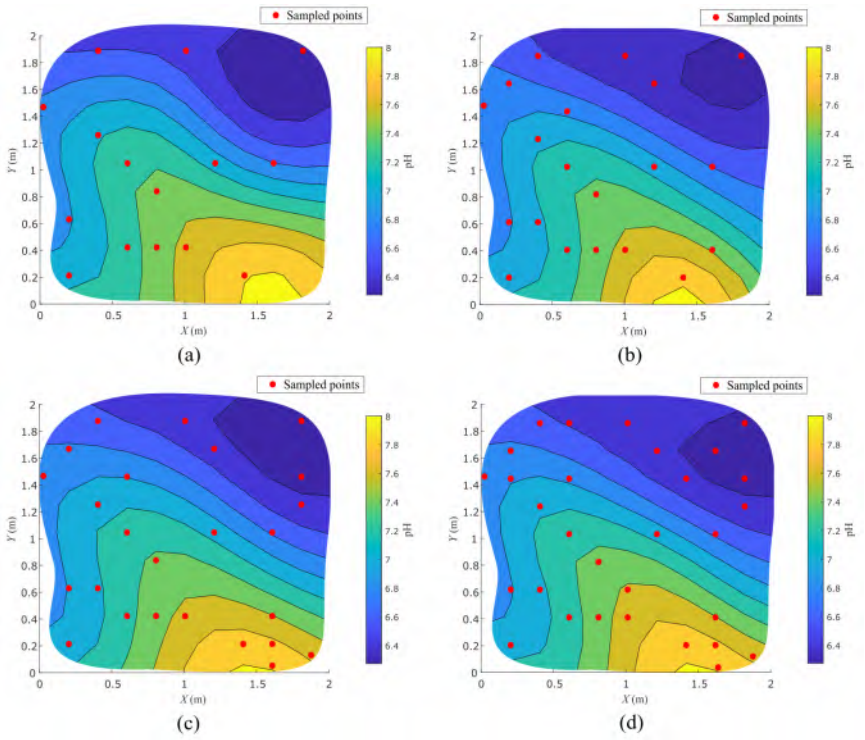

Figure 3.3: Assessing the kriging method accuracy to the fabricated lake by increasing the sampled points showing (a) 15 points, (b) 20 points, (c) 25 points, (d) 30 points.

Rigorous numerical validation illuminated kriging's robust performance, effectively capturing pH distribution within the fabricated lake. Notably, a direct correlation linked kriging accuracy to the count of sampled points [29].

Table 3.1 presents the analysis of absolute mean error, root mean square error (RMSE), and maximum error for the Kriging method.

The values in the table represent the average results from 100 iterations, where each iteration involved different sampled point locations.

The absolute mean error values range from 0.36 (4 points) to 0.16 (30 points), showcasing the variability in error metrics across various numbers of sampled points. Similarly, the RMSE varies from 0.46 to 0.22, and the maximum error ranges from 0.91 to 0.59, illustrating how these error metrics change with the number of sampled points in this comprehensive analysis.

Table 3.1: Mean error, RMSE, and maximum error analysis between the fabricated lake and Kriging method with various sampled points.

Number of Sampled Points	Mean Absolute Error	RMSE	Maximum Error
4	0.36	0.46	0.91
6	0.32	0.41	0.86
8	0.28	0.36	0.81
10	0.25	0.33	0.77
15	0.22	0.29	0.71
20	0.20	0.26	0.66
25	0.18	0.24	0.62
30	0.16	0.22	0.59

Figure 3.4 illustrates the maximum error, absolute mean error, and root mean square error (RMSE) as they vary with the number of sampled points.

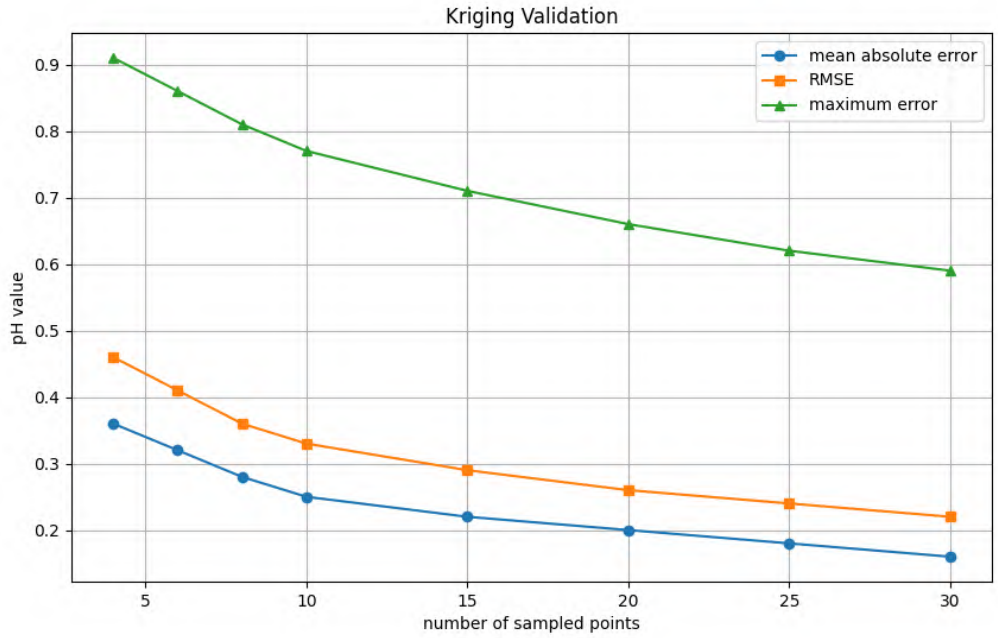

Figure 3.4: Analyzing error metrics across sampled points: maximum error, mean error, and RMSE.

Examining these metrics informs our data quality and sampling strategy decisions. The study confirms kriging's effectiveness in predicting water quality in lakes due to its ability to capture complex spatial patterns.

Sensors Validation

The study carried out a comprehensive benchtop examination aimed at verifying the accuracy of the pH, TDS, turbidity, and temperature sensors through rigorous calibration processes.

Utilizing the dependable VIVOSUN industrial sensors, as exemplified in Figures 3.5 (a) and (b), as reference points, the results revealed remarkably low error percentages, with pH calibration exhibiting a mere 1.34% deviation and TDS calibration showing a similarly impressive 5.23% variance.

The calibration procedure for the ATLAS Scientific pH sensor was particularly meticulous, involving the use of pH 4.00, 7.00, and 10.00 solutions, consistently yielding values that closely aligned with the specified standards.

Temperature measurements were conducted by comparing the DS18B20 sensor to a K-type thermocouple, as illustrated in Figure 3.5 (c), and the findings showcased an outstandingly low error percentage of just 0.81% as outlined in Table 3.2.

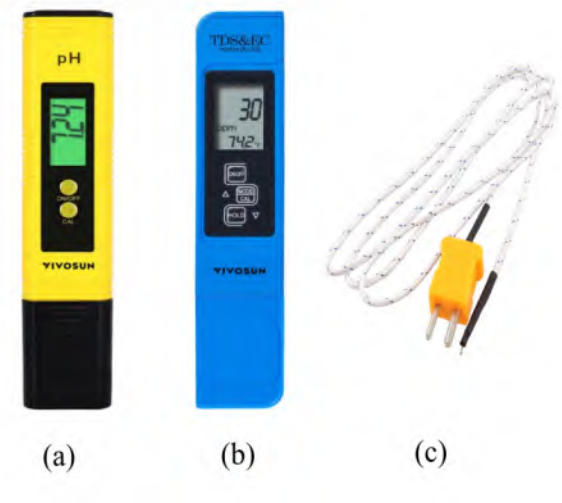

Figure 3.5: (a) Vivosun pH Reference Sensor, (b) Vivosun TDS Reference Sensor, and (c) K-Type Thermocouple Reference Sensor.

Table 3.2: Mean Error Analysis between the Sensor Package Sensors and Reference Sensors.

Parameters	Sensor package value	Reference Sensor Value	Mean Error (%)
pH	6.62	6.71	1.34%
TDS	181	172	5.23%
Temperature	25	24.8	0.81%

To ensure precision in turbidity measurements, the sensor package algorithm integrated a linear function for calibration purposes, resulting in highly accurate readings across the 0 to 100 NTU range. In conclusion, these meticulous calibration procedures and their associated outcomes unquestionably confirm the sensor package's reliability and accuracy in assessing essential water quality parameters.

UAV deploying mechanism validation

To validate the reliability and precision of the sensor package deployment mechanism, a meticulous testing protocol was executed.

The process commenced by securely attaching the sensor package to the UAV's electromagnet, which was, in turn, firmly attached to a metal grip on the surface of the sensor package, ensuring a robust connection.

Figure 3.6 provides a visual representation of the deployment testing process, showcasing its efficiency and accuracy.

This series of images captures the sensor package being deployed into a controlled water-filled flume, designed to replicate real-world aquatic conditions.

These tests exposed the system to intricate aquatic scenarios, enabling a comprehensive evaluation of its performance.

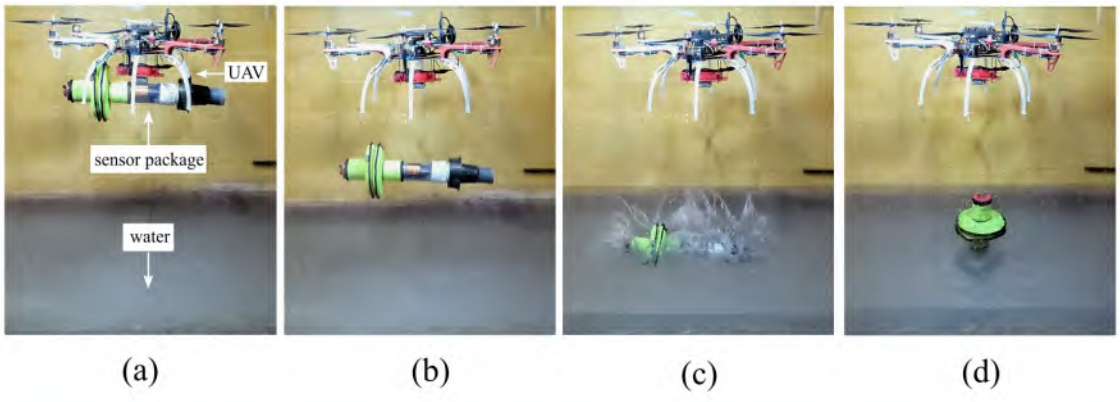

Figure 3.6: Testing of the deployment mechanism to validate real-world reliability showing (a) UAV carrying the sensor package, (b) Releasing sensor package, (c) Sensor package dropped into the water, (d) Sensor package achieves stable floating position.

In addition to these tests, buoyancy aids were incorporated to keep the sensor package afloat on the water's surface, and an anchor mechanism was integrated to maintain its stable position once submerged.

These precise procedures collectively ensured the dependability of the sensor package and its ability to function effectively in demanding environments. The results of this rigorous testing regimen underscored the sensor package's resilience, confirming its readiness for deployment in challenging scenarios and validating its suitability for critical data-gathering missions in dynamic aquatic settings.

Chapter 4

Results

4.1 Kriging Results

In this study, we conducted a comprehensive experiment to assess the water quality of a stationary pond using an in-situ water quality sensor package. Our analysis involved the measurement of crucial parameters, namely pH, total dissolved solids (TDS), turbidity, and temperature, achieved through the deployment of sensors at six strategic locations within the stationary pond, as depicted in Figure 4.1. Rigorous data collection was carried out at each of these designated sampling points, involving the gathering of multiple samples. This meticulous approach enabled us to compute mean values, providing a robust representation of the water quality at each sampled location.

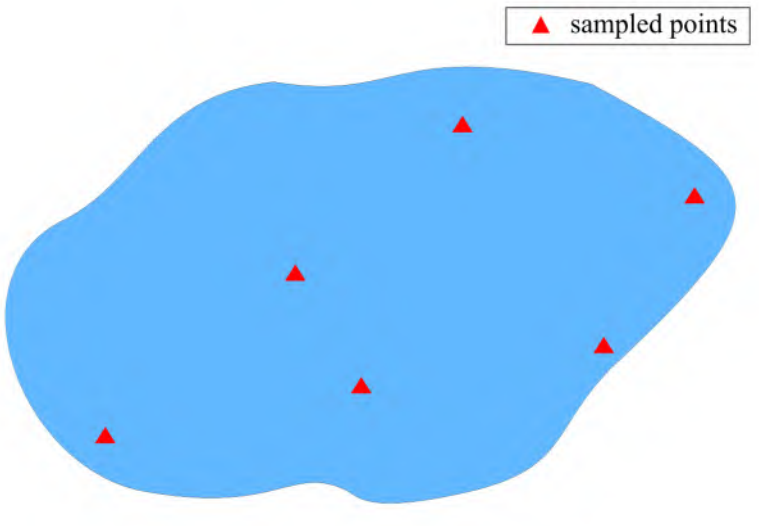

Figure 4.1: Displaying the sampled points within the stationary testing pond.

Additionally, the study employed a kriging process to carefully examine the spatial distribution of these essential water quality parameters across the entire expanse of the stationary pond. By leveraging the collected data, this geostatistical method not only assessed the variability of pH, TDS, turbidity, and temperature within our measured locations but also extrapolated estimated values for unmeasured locations within the pond [16].

For enhanced clarity and visualization, Figure 4.2 illustrates both the stationary pond under investigation and the deployment of our sensor package on the water surface during the data collection process, offering an intuitive understanding of our data collection methodology and vividly illustrating the spatial distribution of water quality parameters within the stationary pond [18].

Figure 4.2: (a) The sensor package floating on the water surface while collecting data, (b) Showcasing the stationary testing pond for the sensor package.

The kriging interpolation plots for TDS, pH, turbidity, and temperature are presented below in Figure 4.3, revealing subtle gradients attributed to the pond's stationary conditions during measurements. Limited water movement gives rise to nuanced variations in TDS, pH, turbidity, and temperature across the pond, providing valuable insights into their spatial distribution.

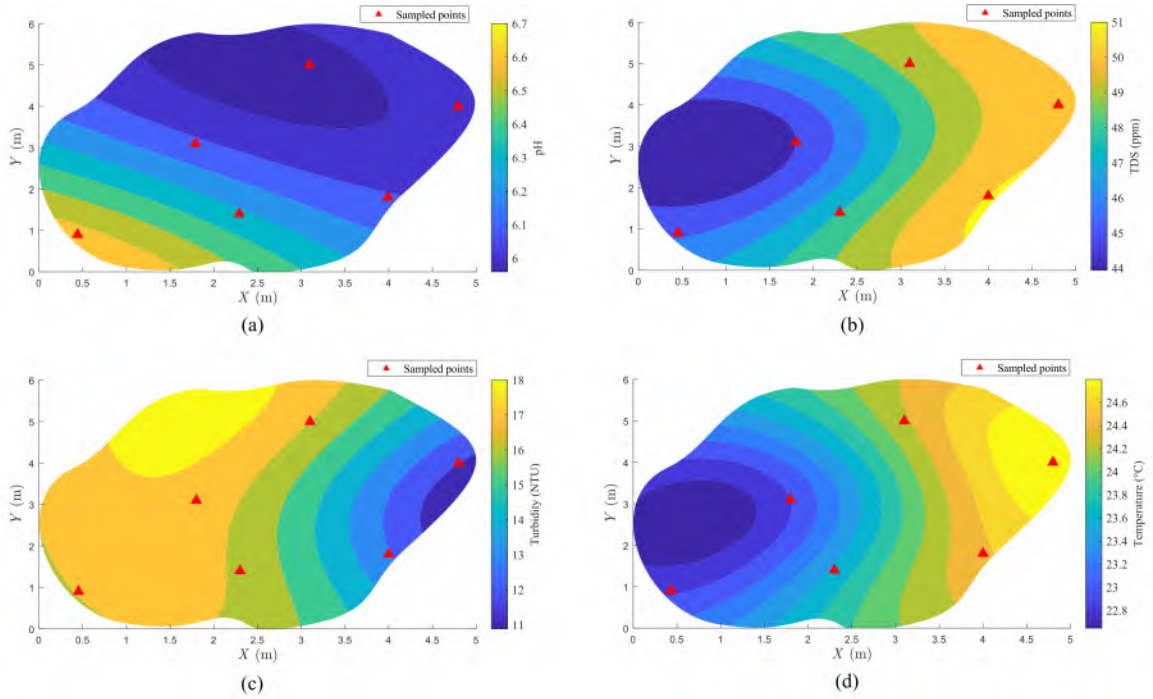

Figure 4.3: Kriging results from onsite testing for water quality mapping showing (a) pH, (b) TDS, (c) turbidity, and (d) temperature.

The TDS plot indicates a gentle gradient from the pond's bottom left to the top right. Elevated TDS levels on the right side result from intensified evaporation driven by increased temperatures in that region. Evaporation concentrates dissolved solids, leading to higher TDS readings. However, TDS values do not directly influence pH or temperature distribution.

Turbidity is heightened on the left side, primarily due to the presence of algae in the bottom left corner. Additionally, the significant accumulation of fallen leaves in the top left corner can notably impact turbidity. As leaves decompose, they release fine particles, organic matter, and other substances into the water, contributing to increased cloudiness. The presence of algae further enhances turbidity as they grow and propagate, releasing particles and affecting water clarity.

Significantly, the bottom left corner exhibits elevated pH levels, primarily attributed to dense algal populations and their photosynthesis activity. Algae release oxygen into the water, raising pH values and creating localized conditions that drive the observed pH increase.

Furthermore, the right side experiences higher temperatures due to intensified sunlight exposure. This condition leads to enhanced evaporation rates and consequent elevations in TDS levels.

The elevated pH in the bottom left corner is primarily due to flourishing algae and their photosynthesis activity. Turbidity is more pronounced on the left side, influenced by both algae and the significant impact of decomposing fallen leaves, which are more concentrated in the top left corner. The right side, with concentrated sunlight, experiences higher temperatures, contributing to elevated TDS levels.

In conclusion, these kriging interpolation plots, as depicted in Figure 4.3, illuminate the nuanced spatial variations in TDS, pH, turbidity, and temperature within the stationary pond, reflecting the intricate dynamics influenced by factors such as sunlight exposure, algae presence, and organic matter decomposition. These insights deepen our understanding of the pond's water quality and its response to its static environment.

4.2 Powermanagement Results

To ensure the reliability and extended operational capability of the sensor package, a comprehensive power management test was conducted under conditions mirroring real-world scenarios. The sensor package was strategically deployed in a stationary pond, as we used for kriging.

For this test, the sensor package was securely anchored to the bottom of the stationary pond, ensuring it was fully immersed and exposed to the elements, just as it would be during operational use in natural aquatic environments as shown in Figure 4.4.

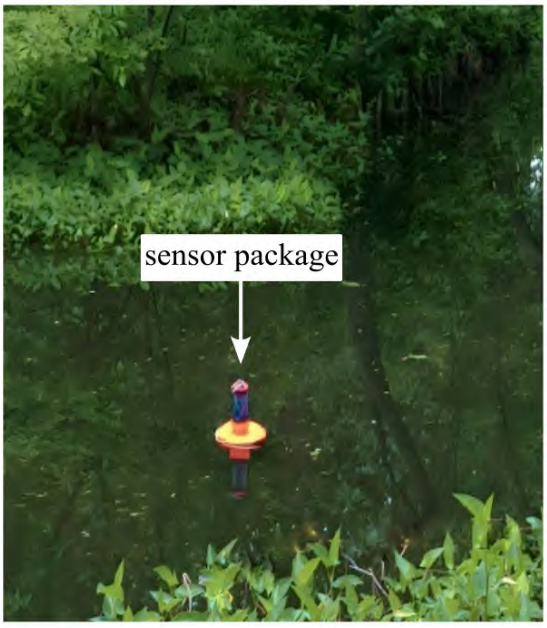

Figure 4.4: Sensor package collecting samples during power management test.

The in-situ water quality sensor package was powered by a 7.4V 1000mAh battery. The test results revealed an impressive operational duration of 32 hours and 48 minutes, highlighting the sensor package's remarkable capability for continuous data collection in such conditions.

Figure 4.5, included below, provides a visual representation of the power management test, illustrating the uninterrupted operation of each sensor throughout the duration of the test. This visual representation emphasizes the sustained functionality and unwavering reliability of the sensor package under these demanding conditions.'

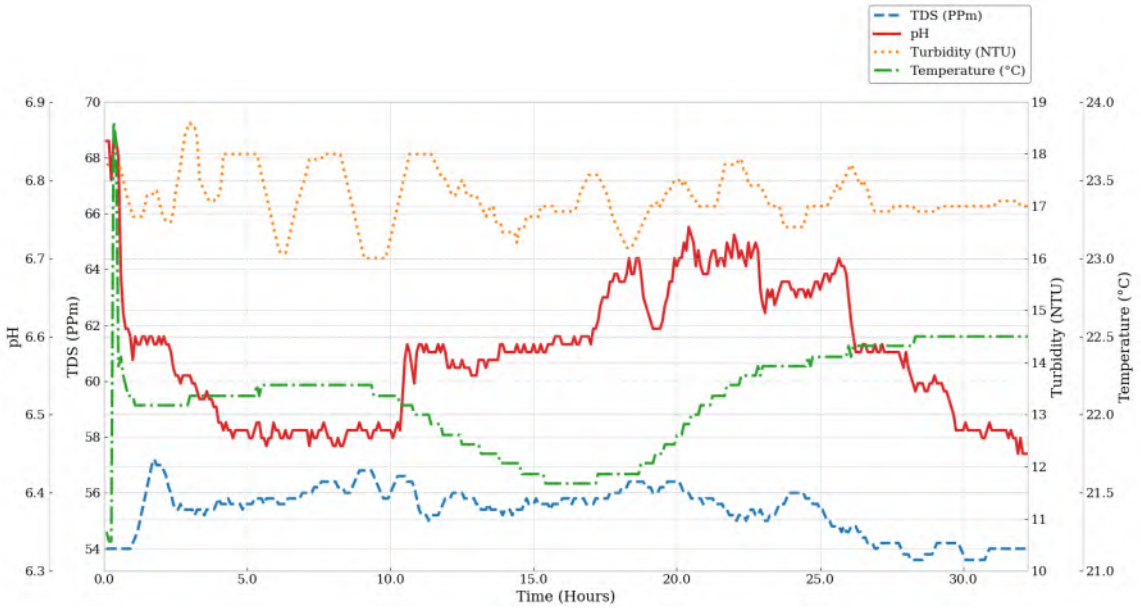

Figure 4.5: Unveling sensor package performance through power management testing.

These findings underscore the robust nature of the sensor package's power management system, which enables extended, uninterrupted data collection in stationary pond environments. This capability has significant implications for long-term monitoring applications, offering a reliable tool for continuous water quality assessment in static aquatic conditions.

4.3 Dynamic Environment Testing Results

A comprehensive test was conducted to evaluate the sensor package's ability to operate effectively in dynamic environments that simulated real-world scenarios with varying conditions. The sensor package was deployed in a creek with continuous water flow, as shown in Figure 4.6 (b), replicating dynamic environmental conditions.

For this test, the sensor package was securely fastened to a sturdy bridge structure using a robust steel wire, allowing it to be positioned within the creek's flowing waters.

This deployment approach ensured that the sensor package was fully immersed, subject to the varying currents, and exposed to the elements, mimicking its operational conditions in natural aquatic environments, as displayed in Figure 4.6 (a).

The in-situ water quality sensor package was powered by a 7.4V 1000mAh battery. The test results revealed an impressive operational duration of 32 hours and 48 minutes, highlighting the sensor package's remarkable capability for continuous data collection in dynamic environments.

Figure 4.6: (a) Sensor package deployed in dynamic environmental conditions, (b) View of the creek utilized for dynamic environment testing

Figure 4.7, included below, provides a visual representation of the dynamic environment test, illustrating the uninterrupted operation of each sensor throughout the duration of the test. This visual representation emphasizes the sensor package's sustained functionality and unwavering reliability under these demanding conditions.

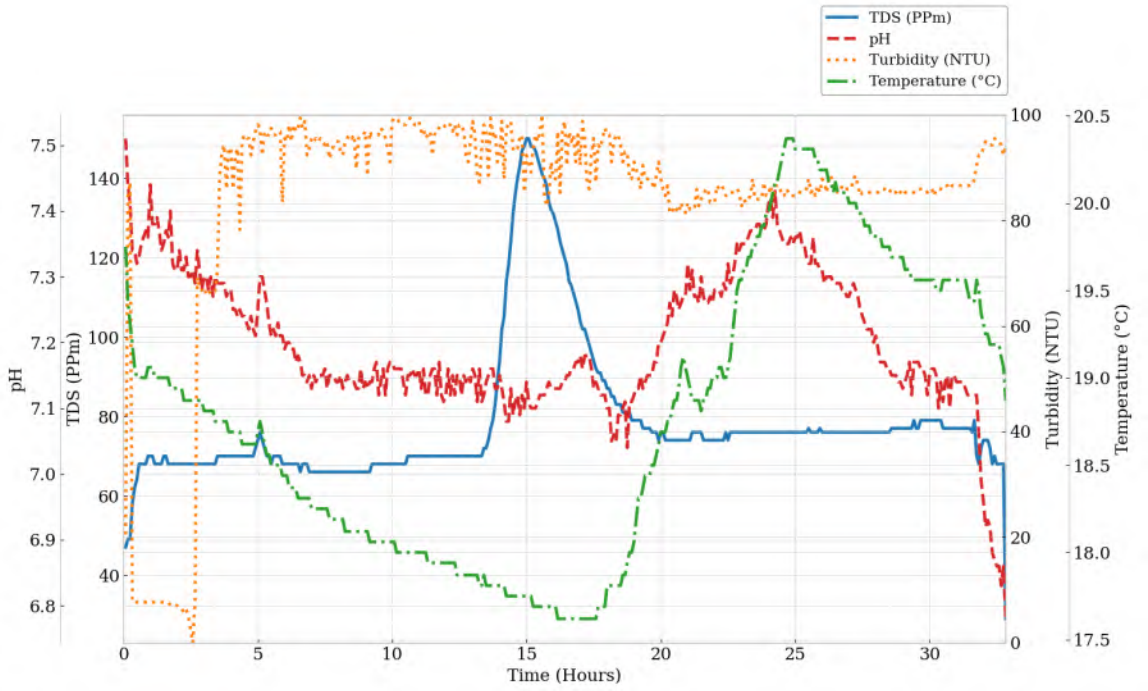

Figure 4.7: Assessing sensor package performance in dynamic environments.

These findings underscore the robust nature of the sensor package's operational capability in dynamic environments, making it a reliable tool for continuous data collection in ever-changing aquatic conditions. This capability has significant implications for applications such as long-term monitoring of water quality, where reliable performance in dynamic environments is essential.

Chapter 5

Conclusion

Integrating real-time automated water quality testing and spatial kriging, in conjunction with the innovative utilization of a UAV (Unmanned Aerial Vehicle) for efficient data collection, offers a highly efficient and cost-effective method for accurately mapping water quality parameters. This system, combining in-situ sensors, UAV, and real-time monitoring capabilities, provides reliable information on water quality conditions. The precise spatial representation offered by kriging enables effective interventions and informed decision-making to maintain and improve water quality. To ensure reliability, the in-situ water quality sensor package is securely attached to a floating surface, providing flotation. It is highly waterproofed for operation in severe weather and various environmental conditions. Extensive testing in different locations within a stationary pond validated the package's effectiveness, improving real-time monitoring of water quality parameters such as pH, turbidity, total dissolved solids (TDS), and temperature. The sensor package incorporates a high-power-saving system capable of continuous operation for 32 hours and 48 minutes. This duration provides an adequate period to track fluctuations that may occur within minutes to hours due to weather conditions, solar radiation, and biological activity, which influence water quality parameters. Future research will focus on implementing GPS into the embedded system to provide highly accurate coordinates for improved kriging, as well as incorporating a more accurate optimal sensor placement method. Additionally, including PV solar panels will extend the system's operating time, considering the potential impact of the GPS implementation.

Bibliography

[1] Ahmed AH Al-Fahdawi, Adel M Rabee, and Shaheen M Al-Hirmizy, *Water quality monitoring of al-habbaniyah lake using remote sensing and in situ measurements*, Environmental monitoring and assessment **187** (2015), 1–11.

[2] Fhranz Marc Lou S. Alimorong, Haziel Anne D. Apacionado, and Jocelyn Flores Villaverde, *Arduino-based multiple aquatic parameter sensor device for evaluating ph, turbidity, conductivity and temperature*, 2020 IEEE 12th International Conference on Humanoid, Nanotechnology, Information Technology, Communication and Control, Environment, and Management (HNICEM), 2020, pp. 1–5.

[3] Juan G Arango and Robert W Nairn, *Prediction of optical and non-optical water quality parameters in oligotrophic and eutrophic aquatic systems using a small unmanned aerial system*, Drones **4** (2019), no. 1, 1.

[4] Bikram Pratap Banerjee, Simit Raval, Thomas J Maslin, and Wendy Timms, *Development of a uav-mounted system for remotely collecting mine water samples*, International Journal of Mining, Reclamation and Environment **34** (2020), no. 6, 385–396.

[5] Richard H Becker, Michael Sayers, Dustin Dehm, Robert Shuchman, Kaydian Quintero, Karl Bosse, and Reid Sawtell, *Unmanned aerial system based spectroradiometer for monitoring harmful algal blooms: A new paradigm in water quality monitoring*, Journal of Great Lakes Research **45** (2019), no. 3, 444–453.

[6] Patricia A Beddows and Edward K Mallon, *Cave pearl data logger: A flexible arduino-based logging platform for long-term monitoring in harsh environments*, Sensors **18** (2018), no. 2, 530.

[7] Kirk Cameron and Philip Hunter, *Using spatial models and kriging techniques to optimize long-term ground-water monitoring networks: a case study*, Environmetrics: The official journal of the International Environmetrics Society **13** (2002), no. 5-6, 629–656.

[8] Sabrina Carroll, Michail Kalaitzakis, and Nikolaos Vitzilaios, *Uas sensor deployment and retrieval to the underside of structures*, 2021 International Conference on Unmanned Aircraft Systems (ICUAS), IEEE, 2021, pp. 895–900.

[9] André Tristany Farinha, Julien di Tria, Marta Reyes, Constanca Rosas, Oscar Pang, Raphael Zufferey, Francesco Pomati, and Mirko Kovac, *Off-shore and underwater sampling of aquatic environments with the aerial-aquatic drone medusa*, Frontiers in Environmental Science **10** (2022), 2305.

[10] CT Graham, I O'Connor, L Broderick, M Broderick, O Jensen, and HT Lally, *Drones can reliably, accurately and with high levels of precision, collect large volume water samples and physio-chemical data from lakes*, Science of The Total Environment **824** (2022), 153875.

[11] Wong Jun Hong, Norazanita Shamsuddin, Emeroylariffion Abas, Rosyzie Anna Apong, Zarifi Masri, Hazwani Suhaimi, Stefan Herwig Gödeke, and Muhammad Nafi Aqmal Noh, *Water quality monitoring with arduino based sensors*, Environments **8** (2021), no. 1, 6.

[12] Wonse Jo, Yuta Hoashi, Lizbeth Leonor Paredes Aguilar, Mauricio Postigo-Malaga, José M Garcia-Bravo, and Byung-Cheol Min, *A low-cost and small usv platform for water quality monitoring*, HardwareX **6** (2019), e00076.

[13] Cengiz Koparan, Ali Bulent Koc, Charles V Privette, and Calvin B Sawyer, *Autonomous in situ measurements of noncontaminant water quality indicators and sample collection with a uav*, Water **11** (2019), no. 3, 604.

[14] Vinod Kothari, Suman Vij, SuneshKumar Sharma, and Neha Gupta, *Correlation of various water quality parameters and water quality index of districts of uttarakhand*, Environmental and Sustainability Indicators **9** (2021), 100093.

[15] Damir Krkljes, Goran Kitic, Csaba Petes, Slobodan Birgermajer, Jovana Stanojev, Branimir Bajac, Marko Panic, Vasa Radonic, Ilija Brceski, Rok Stravs, et al., *Multiparameter water quality monitoring system for continuous monitoring of fresh waters*, arXiv preprint arXiv:2307.11630 (2023).

[16] Geoffrey M Laslett, *Kriging and splines: an empirical comparison of their predictive performance in some applications*, Journal of the American Statistical Association **89** (1994), no. 426, 391–400.

[17] Ying Lo, Lang Fu, Tiancheng Lu, Hong Huang, Lingrong Kong, Yunqing Xu, and Cheng Zhang, *Medium-sized lake water quality parameters retrieval using multispectral uav image and machine learning algorithms: A case study of the yuandang lake, china*, Drones **7** (2023), no. 4, 244.

[18] Tain-Shing Ma, Marios Sophocleous, and Yun-Sheng Yu, *Geostatistical applications in ground-water modeling in south-central kansas*, Journal of Hydrologic Engineering **4** (1999), no. 1, 57–64.

[19] Ryan McEliece, Shawn Hinz, Jean-Marc Guarini, and Jennifer Coston-Guarini, *Evaluation of nearshore and offshore water quality assessment using uav multispectral imagery*, Remote Sensing **12** (2020), no. 14, 2258.

[20] Rebecca R Murphy, Frank C Curriero, and William P Ball, *Comparison of spatial interpolation methods for water quality evaluation in the chesapeake bay*, Journal of Environmental Engineering **136** (2010), no. 2, 160–171.

[21] Vasant Raj Mutha, Narendra Kumar, and Parikshit Pareek, *Real time standalone data acquisition system for environmental data*, 2016 IEEE 1st International Conference on Power Electronics, Intelligent Control and Energy Systems (ICPEICES), 2016, pp. 1–4.

[22] R Nagalakshmi, K Prasanna, S Prakash Chandar, et al., *Water quality analysis using gis interpolation method in serthalaikadu lagoon, east coast of india*, Rasayan Journal of Chemistry **9** (2016), no. 4, 634–640.

[23] Margaret A Oliver and Richard Webster, *Kriging: a method of interpolation for geographical information systems*, International Journal of Geographical Information System **4** (1990), no. 3, 313–332.

[24] John-Paul Ore, Sebastian Elbaum, Amy Burgin, and Carrick Detweiler, *Autonomous aerial water sampling*, Journal of Field Robotics **32** (2015), no. 8, 1095–1113.

[25] Sami O Osman, Mohamed Z Mohamed, Alzain M Suliman, and Amjed A Mohammed, *Design and implementation of a low-cost real-time in-situ drinking water quality monitoring system using arduino*, 2018 International Conference on Computer, Control, Electrical, and Electronics Engineering (ICCCEEE), IEEE, 2018, pp. 1–7.

[26] Reagan Helen Pearce, *Do-it-yourself": evaluating the potential of arduino technology in monitoring water quality*, Unpublished Bachelor's dissertation. doi **10** (2018).

[27] Aravinda S Rao, Stephen Marshall, Jayavardhana Gubbi, Marimuthu Palaniswami, Richard Sinnott, and Vincent Pettigrovet, *Design of low-cost autonomous water quality monitoring system*, 2013 International Conference on Ad-

vances in Computing, Communications and Informatics (ICACCI), IEEE, 2013, pp. 14–19.

[28] Paulo Rodrigues, Francisco Marques, Eduardo Pinto, Ricardo Pombeiro, André Lourenço, Ricardo Mendonça, Pedro Santana, and José Barata, *An open-source watertight unmanned aerial vehicle for water quality monitoring*, OCEANS 2015-MTS/IEEE Washington, IEEE, 2015, pp. 1–6.

[29] S Sakata, F Ashida, and M Zako, *An efficient algorithm for kriging approximation and optimization with large-scale sampling data*, Computer methods in applied mechanics and engineering **193** (2004), no. 3-5, 385–404.

[30] Kazi Ragib Ishraq Sanim, Caitlyn English, Zechariah B Kitzhaber, Michail Kalaitzakis, Nikolaos Vitzilaios, Michael L Myrick, Michael E Hodgson, and Tammi L Richardson, *Autonomous uas-based water fluorescence mapping and targeted sampling*, Journal of Intelligent & Robotic Systems **108** (2023), no. 2, 25.

[31] Tahoora Sheikhy Narany, Mohammad Firuz Ramli, Ahmad Zaharin Aris, Wan Nor Azmin Sulaiman, and Kazem Fakharian, *Spatial assessment of groundwater quality monitoring wells using indicator kriging and risk mapping, amol-babol plain, iran*, Water **6** (2013), no. 1, 68–85.

[32] Brian J Straight, Devin N Castendyk, Diane M McKnight, Connor P Newman, Pierre Filiatreault, and Americo Pino, *Using an unmanned aerial vehicle water sampler to gather data in a pit-lake mining environment to assess closure and monitoring*, Environmental Monitoring and Assessment **193** (2021), no. 9, 572.

[33] Mercedes Vélez-Nicolás, Santiago García-López, Luis Barbero, Verónica Ruiz-Ortiz, and Ángel Sánchez-Bellón, *Applications of unmanned aerial systems (uass) in hydrology: A review*, Remote Sensing **13** (2021), no. 7, 1359.

[34] Irina Yaroshenko, Dmitry Kirsanov, Monika Marjanovic, Peter A Lieberzeit, Olga Korostynska, Alex Mason, Ilaria Frau, and Andrey Legin, *Real-time water quality monitoring with chemical sensors*, Sensors **20** (2020), no. 12, 3432.